Hindawi
Journal of Nanomaterials
Volume 2019, Article ID 5602742, 7 pages
https://doi.org/10.1155/2019/5602742

Research Article

Effect of Pretreatment on Magnetic Nanoparticle Growth on Graphene Surface and Magnetic Performance in Electroless Plating

Kyunbae Lee, Taehoon Kim, Sang Bok Lee, and Byung Mun Jung

Composites Research Division, Korea Institute of Materials Science, Changwon 51508, Republic of Korea

Correspondence should be addressed to Taehoon Kim; tkim67@kims.re.kr and Byung Mun Jung; bmjung@kims.re.kr

Received 30 August 2018; Revised 12 December 2018; Accepted 23 December 2018; Published 18 March 2019

Academic Editor: Philip D. Rack

Electroless plating involves sensitization, activation, and plating processes. Sensitization and activation are conducted by dipping the substrate in $SnCl_2$ solution and $PdCl_2$ solution, respectively. These pretreatment processes are required to plate the substrate with noncatalytic surfaces. We investigated the effect of sensitization on the magnetic properties of FeCoNi@graphene hybrids prepared via electroless plating. The solution concentrations during sensitization were varied to observe changes in the structural, morphological, and magnetic properties of FeCoNi@graphene using XRD, TEM, and VSM, respectively. Sensitization under high concentration produced a large amount of SnO_2, resulting in low saturation magnetization. Further, the FeCoNi@graphene hybrid prepared via electroless plating without sensitization also exhibited low saturation magnetization owing to the formation of oxides and hydroxides. We prepared FeCoNi@graphene with a saturation magnetization of 40.8 emu/g under sensitization at low concentration; this is the highest saturation magnetization among the reported magnetic material@graphene hybrids prepared via electroless plating. This study provides guidelines for the pretreatment of graphene via electroless plating and should contribute to future studies on the synthesis of magnetic material@graphene hybrids.

1. Introduction

Soft magnetic alloys are used in electromagnetic absorbers [1, 2], transformers [3], and magnetic sensors [4, 5] owing to their satisfactory soft magnetic properties including high saturation magnetization, low coercivity, and high permeability [6–9]. When magnetic materials are hybridized using graphene, the combination of the recoverable characteristics of the magnetic material and the surface characteristics of graphene can maximize their utility in various applications such as recoverable catalysts [10, 11]. Magnetic material@graphene hybrids are synthesized using various chemical methods [12–16]. However, additional reduction processes are required to obtain hybrid materials of graphene and metallic magnetic materials with higher saturation magnetization [1, 11, 13, 17].

Electroless plating is widely used in the industry to prepare metal-coated substrates because it affords several advantages: (1) it does not require external power, unlike the electroplating method; (2) a material can be coated on an insulating substrate; and (3) metals can be coated on a substrate without an additional reduction process, unlike in other chemical synthesis methods. Studies have been conducted regarding electroless plating to grow metal nanoparticles on graphene without heat treatment [13, 15, 18–20]. For example, nanoparticles of noble metals such as Pt, Pd, Au, and Ag have been grown on graphene via electroless plating [14, 16, 18, 21–23]. Recently, magnetic particles including nickel [24] and nickel cobalt nanoparticles [21] were grown on graphene by electroless plating. Therefore, electroless plating can be used to prepare magnetic metal@graphene hybrids without heat treatment.

Electroless plating involves three steps: sensitization, activation, and plating. During sensitization and activation, tin and Pd are grown on the substrate; Pd is used as a catalyst. The effect of sensitization on the electroless plating of conventional materials was well reviewed by Wei and Roper [25]. However, the effect of sensitization on the electroless

plating of graphene should be different from that for conventional macroscale materials. For the latter, the amounts of tin, Pd, and plated metal are much smaller than that of the substrate, whereas for the former, these amounts could be greater than that of graphene owing to the high specific surface area of graphene. In particular, if excess tin and Pd are produced on the graphene surface during the pretreatment processes, the saturation magnetization of the magnetic metal@graphene hybrids will decrease because tin and Pd have low magnetism. Therefore, it is reasonable to assume that pretreatments for electroless plating would affect the magnetic properties of the magnetic metal nanoparticle@graphene. Although certain studies have investigated metal@graphene hybrids prepared via electroless plating, few studies have analyzed the effect of pretreatments on graphene.

In this study, we investigated the effect of sensitization on FeCoNi@graphene hybrids synthesized by electroless plating. FeCoNi was selected because of the high saturation magnetization of FeCo and high corrosion stability of Ni. The atomic ratio of Fe : Co : Ni is 13 : 77 : 10, which was used in our previous work for the electroless plating of FeCoNi on the surface of carbon fibers (CFs) [2]. We prepared a series of sensitized graphenes by controlling the concentration of the sensitizing solutions. The FeCoNi@graphene hybrids were structurally and magnetically analyzed by transmission electron microscopy (TEM), X-ray diffraction (XRD), and with a vibrating sample magnetometer (VSM). It was observed that excess sensitization induces a large amount of SnO_2 nanoparticles and increases the overall mass, thereby reducing the saturation magnetization. Further, sensitization-free FeCoNi@graphene hybrids demonstrated low saturation magnetization, indicating that sensitization is required to grow highly magnetic metals. When the FeCoNi@graphene hybrid was prepared under the lowest sensitization concentration, the saturation magnetization of the hybrid was 40.8 emu/g, which is the highest saturation magnetization among the reported magnetic@graphene hybrids prepared by electroless plating. This study provides chemical insights into the electroless plating of metal nanoparticle@graphene hybrids for realizing the mass production of functional magnetic hybrids.

2. Materials and Methods

2.1. Electroless Plating. Before electroless plating, sensitization and activation are required. First, 100 ml of water-dispersed graphene paste (2 wt%, Mexplorer) was sensitized in 1,000 ml of $SnCl_2$ (98%, Alfa Aesar) aqueous solutions (pH 1) for 30 min at 45°C. The water-dispersed graphene was partially oxidized to allow dispersion in water; nevertheless, it possessed the sp^2 conjugation. Therefore, in this work, it is referred to as "graphene," not graphene oxide. The $SnCl_2$ concentration was varied from 0.2 to 20 g/l. We denote the sensitized graphene treated using the $SnCl_2$ solution with a concentration of n g/l as Sn@G(n). The sensitized graphene was filtered and subsequently activated in 1,000 ml of $PdCl_2$ (Kojima Chemicals Co. Ltd.) aqueous solution (pH 1) with a concentration of 0.2 g/l for 30 min at 45°C.

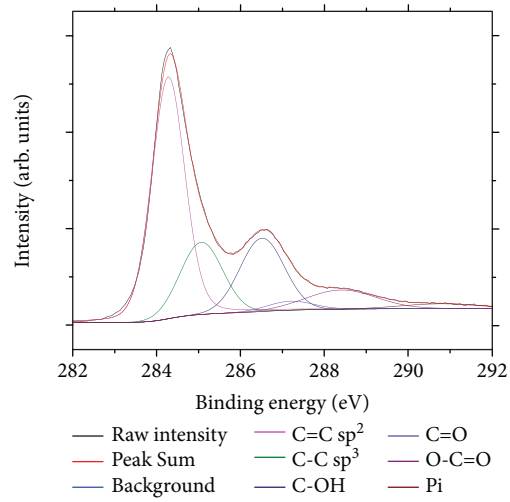

Figure 1: Deconvoluted C1s XPS spectra of graphene used in this experiment.

The activated graphene was obtained by filtering, washing, and dispersing in 500 ml of water. We denote the activated graphene treated by the $PdCl_2$ solution as Pd@G(n). To compare the effects with and without sensitization, we synthesized the Pd-grown graphene without sensitization. Because Pd nanoparticles have rarely been grown on a graphene surface without tin, we used previously reported conditions to achieve this [26]. For this, 100 ml of water-dispersed graphene paste was mixed with 1,000 ml of the H_2PdCl_4 aqueous solution at a concentration of 0.282 g/l for 30 min at 0°C. The sensitization-free activated graphene was denoted as Pd@G(0). The electroless plating solution contained 0.26 M borane dimethylamine complex (DMAB, 97%, Alfa Aesar), 0.2 M sodium tartrate (99%, Alfa Aesar), 0.05 M trisodium citrate (99%, Alfa Aesar), 0.05 M phosphorous acid (97%, Alfa Aesar), 0.2 M ammonium sulfate (98+%, Alfa Aesar), and 0.07 M metal sulfate heptahydrate (cobalt (II) sulfate heptahydrate (Junsei Chemical Co. Ltd.), iron (II) sulfate heptahydrate (Junsei Chemical Co. Ltd.), and nickel (II) sulfate heptahydrate (Sigma-Aldrich), with the molar ratio of Co : Fe : Ni at 77 : 13 : 10). The pH of the plating solution was 6.5, and it was controlled by the addition of sodium hydroxide (>98%, Samchun Chemical Co. Ltd.). A total of 500 ml of the plating solution was mixed with the activated graphene-dispersed suspension and stirred for 30 min at 75°C. After electroless plating, the FeCoNi@graphene hybrid was filtered using a magnetic bar and washed twice. The hybrid materials are denoted as FCN@G(n). The weight ratio of FeCoNi to graphene in FCN@G was 1 : 1 in this experiment.

2.2. Characterizations. The morphologies of the hybrid materials were examined by field-emission scanning electron microscopy (FE-SEM; JEOL JSM-7610F) at an accelerating voltage of 15.0 kV and TEM (Hitachi HF-3300) at an accelerating voltage of 300.0 kV. The saturated magnetization of the hybrid materials was measured using a VSM (7407 Series VSM, Lake Shore Cryotronics Inc.) at room

temperature. The X-ray diffractograms of the FeCoNi@graphene were recorded in the reflection mode, which is a standard procedure for XRD measurements, using Ni-filtered Cu-Kα radiation ($\lambda_f = 0.154184$ nm) on a D/Max 2500 (Rigaku). Thermogravimetric analysis (TGA) was conducted under air flow at the heating rate of 10°C/min using a STARe system (Mettler Toledo). The functional groups were determined by X-ray photoelectron spectroscopy (K-Alpha+ XPS System, Thermo Fisher Scientific).

3. Results and Discussion

The graphene used in this experiment was partially oxidized graphene. Figure 1 shows the hydroxyl and carboxyl groups of the graphene, which enable its dispersion in water. To investigate the effect of the amount of Sn/SnO_2, we first analyzed the ratio of SnO_2 to graphene. This ratio could be obtained via TGA because graphene degrades at approximately 600°C in air (Figure 2(a)). Typically, the concentration of a $SnCl_2$ solution should be high for sensitization. For example, in our previous work, we used 20 g/l of $SnCl_2$ solution to sensitize the surface of CFs. When 20 g/l of sensitization solution was used for graphene, a large amount of residue was obtained after calcination, indicating that several SnO_2 nanoparticles were grown on the graphene surface during sensitization. By contrast, when CFs were sensitized with the same concentration, the ratio of SnO_2 nanoparticles on CFs was considerably smaller than that on graphene. This indicates that Sn precursors grew effectively on the graphene surface. This difference in sensitization between conventional macroscale materials and graphene will lead to different results in electroless plating. In particular, excess SnO_2 increases the mass of the entire hybrid material, thereby reducing the saturation magnetization. Unlike during sensitization, the activation process rarely increases the mass of graphene (Figure 2(b)). Therefore, we focus on investigating the sensitization of graphene to obtain highly magnetized hybrid materials.

We calculated the theoretical ratio of SnO_2 assuming that all $SnCl_2$ was converted into SnO_2. Notably, the experimentally obtained ratio of SnO_2 is similar to the theoretical ratio of SnO_2 when the $SnCl_2$ concentration is 0.2–2 g/l (Figure 2(c)), implying that almost all Sn precursors are grown on the graphene surface. At higher concentration, the experimentally obtained SnO_2 ratio is smaller than the theoretically obtained one because the graphene surface is already covered with SnO_2. TEM images indicate that SnO_2 nanoparticles with sizes of 3-4 nm grew on the graphene surface (Figure 3). While a small amount of SnO_2 nanoparticles was observed in Sn@G(0.2), most of the surface of Sn@G(2) was already covered by SnO_2 nanoparticles; this is in agreement with previous TGA results.

The XRD results demonstrated that the intensity of the (110), (101), and (211) peaks of SnO_2 increased as the $SnCl_2$ concentration increased. In contrast, the (002) peak of graphite was observed when a low-concentration $SnCl_2$ solution was used for sensitization (Figure 4(a)). The (002) graphite peak indicates that Sn@G(0.2) tends to restack and form graphite because the surface coverage of SnO_2 in Sn@G(0.2) is low.

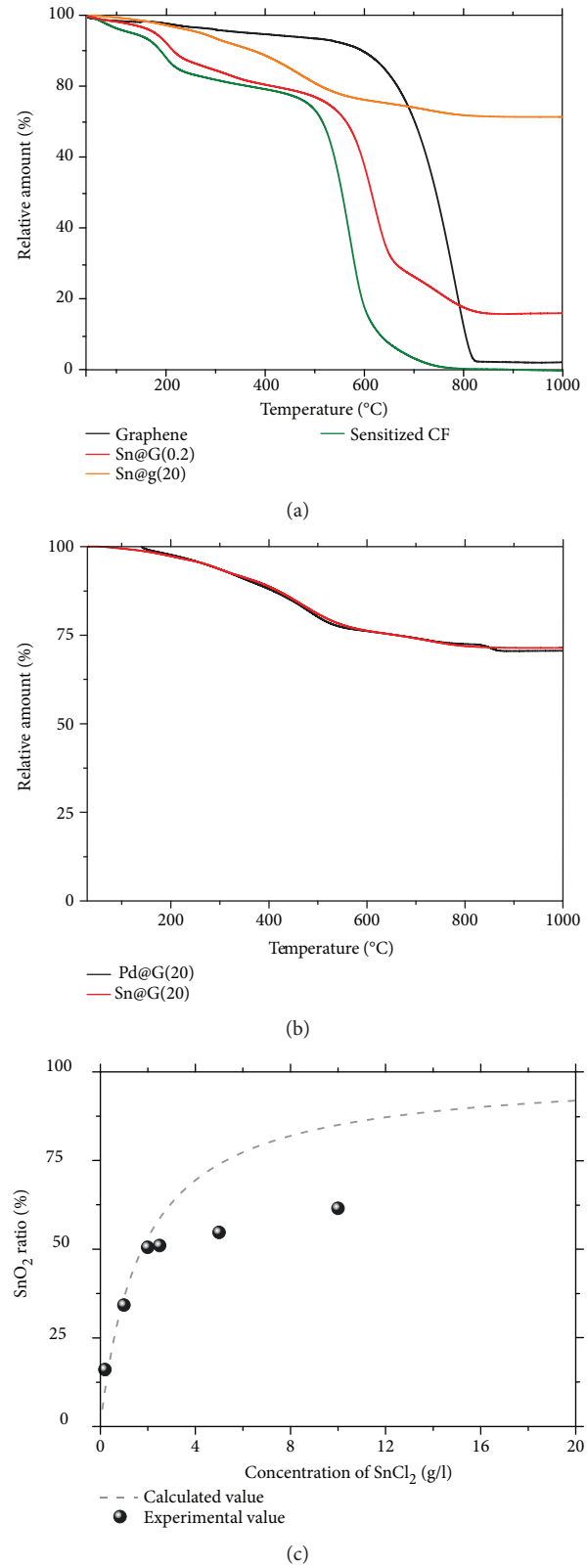

Figure 2: (a) TGA plots of graphene (black), sensitized graphene (red, orange), and sensitized CF prepared using 20 g/l $SnCl_2$ solution (green). (b) TGA plots of sensitized and activated graphene. (c) SnO_2 ratio of sensitized graphene obtained using TGA (circle) and theoretical calculation assuming that all $SnCl_2$ is converted to SnO_2 (dotted line).

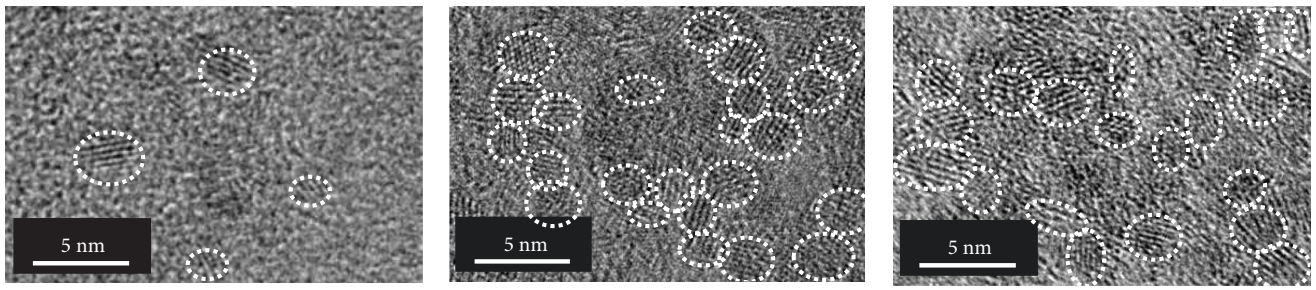

(a) (b) (c)

Figure 3: TEM images of sensitized graphene. (a) Sn@G(0.2), (b) Sn@G(2), and (c) Sn@G(20). The dotted white circles indicate the SnO_2 nanoparticles.

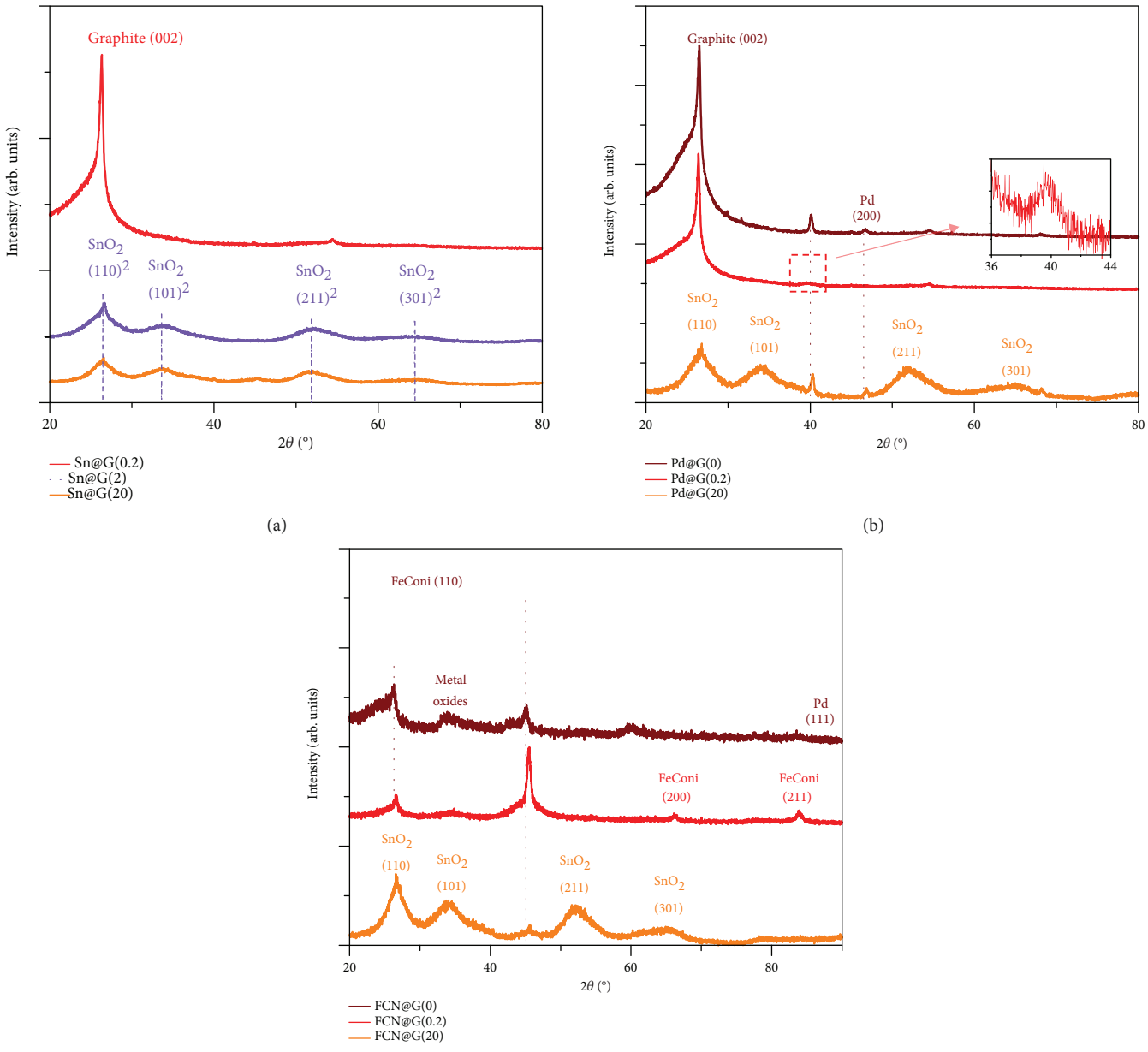

(a) (b) (c)

Figure 4: XRD patterns of (a) sensitized graphene, (b) activated graphene, and (c) FeCoNi@graphene hybrids prepared under different sensitization conditions.

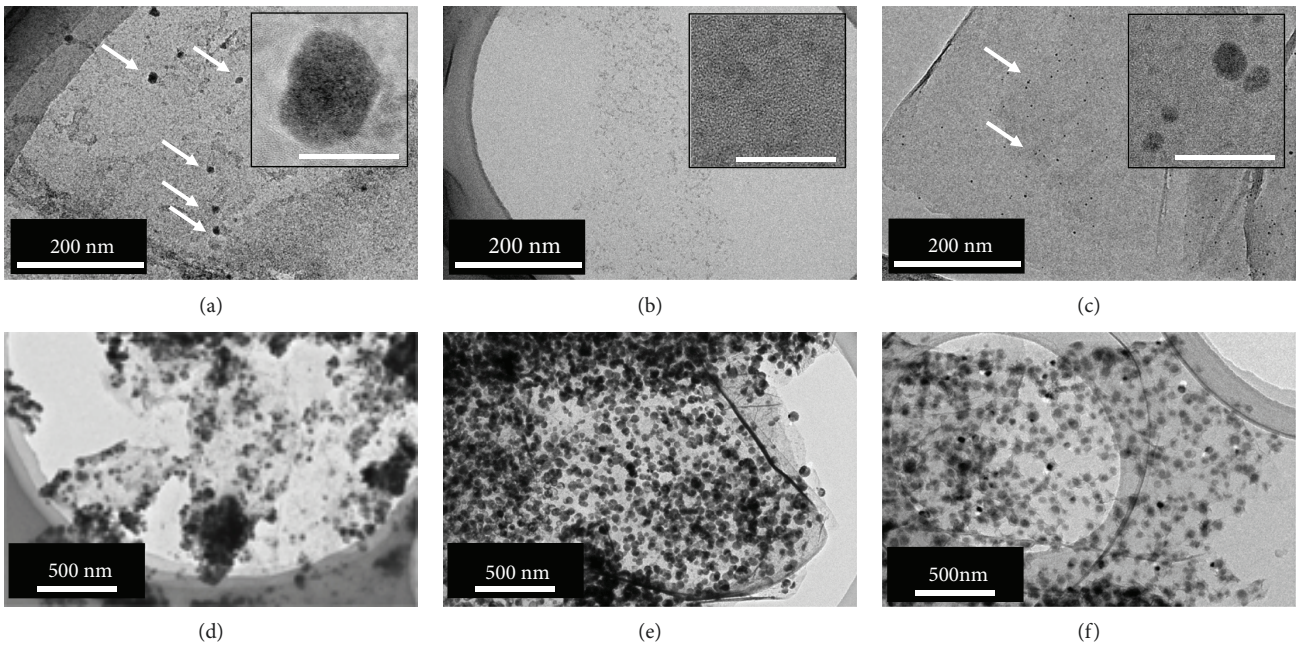

Figure 5: TEM images of activated graphene. (a) Pd@G(20), (b) Pd@G(0.2), (c) Pd@G(0), (inset: magnified images with a scale bar of 15 nm) (d) FCN@G(20), (e) FCN@G(0.2), and (f) FCN@G(0).

Thus, a low-concentration $SnCl_2$ solution is appropriate for increasing the saturation magnetization by reducing excess SnO_2; however, the low surface coverage of SnO_2 may induce restacking and poor Pd growth during activation. Therefore, we prepared three activated graphene samples to observe the effect of the $SnCl_2$ concentration and sensitization: (1) 20 g/l sensitization condition (Pd@G(20)), (2) 0.2 g/l sensitization condition with exceedingly low concentration (Pd@G(0.2)), and (3) sensitization-free activated graphene (Pd@G(0)). The activated graphene samples were analyzed and used for the subsequent plating.

TEM images of Pd@G(20) indicate the growth of large-sized (>20 nm) Pd nanoparticles (Figure 5(a)), which correspond to the sharp Pd (111) peak of Pd@G(20) in the XRD pattern (Figure 4(b)). Small-sized Pd nanoparticles (2-5 nm) are uniformly distributed on the surface of graphene in Pd@G(0) (Figure 5(c)), which correspond to the sharp Pd (111) peak in the XRD pattern (Figure 4(b)). However, it is difficult to observe Pd nanoparticles in the TEM images of Pd@G(0.2) (Figure 5(b)). The gray spots in the inset of Figure 5(b) are SnO_2 particles, not Pd nanoparticles. These correspond to the exceedingly small and broad Pd (111) peak observed in the XRD pattern (Figure 4(b)). To determine which Pd nanoparticles are appropriate for the preparation of a highly magnetic graphene hybrid, plating was conducted using the three Pd@G samples.

After plating, the surface of the FeCoNi@graphene hybrid consisted of FeCoNi nanoparticles and an exposed graphene surface (Figures 5(d)–5(f)); therefore, the hybrid materials are appropriate for demonstrating both the magnetic performance and the features of graphene such as adsorption of pollutants or sensing properties. TEM images indicate that several FeCoNi nanoparticles of FCN@G(20) are aggregated on a specific area (Figure 5(d)). Nonuniformly distributed Pd nanoparticles of Pd@G(20) would produce nonuniformly distributed FeCoNi nanoparticles. Moreover, the crystallinity of the FeCoNi nanoparticles of FCN@G(20) is somewhat low (Figure 4(c)); its peak is even lower than that of the residual SnO_2. In contrast, 20–50 nm-sized FeCoNi nanoparticles are uniformly grown on FCN@G(0.2) and FCN@G(0). Although the Pd nanoparticles of Pd@G(0.2) are not observed in the TEM images, plating was successfully performed. This indicates that exceedingly small Pd nanoparticles were dispersed on the Pd@G(0.2) sample, as shown in the XRD patterns. The FeCoNi nanoparticles of FCN@G(0.2) exhibited a strong BCC (110) peak; thus, low-concentration $SnCl_2$ is appropriate for preparing highly magnetic particles. The FeCoNi nanoparticles of FCN@G(0) are similar in size and shape to those of FCN@G(0.2). However, the XRD pattern shows a broad peak near 32–37°. This peak may have originated from various metal oxides such as $CoFe_2O_4$, $NiFe_2O_4$, and Co_3O_4 [27–29]. It is believed that oxides degrade the magnetic properties.

The saturation magnetization of various FeCoNi@graphene samples was evaluated using a VSM (Figure 6). As expected, the hybrids sensitized at a lower concentration exhibited higher saturation magnetization. However, when sensitization was omitted altogether, the saturation magnetization was lower owing to the formation of oxides and hydroxides. The highest saturation magnetization (40.8 emu/g) was obtained when the concentration of the sensitization solution was 0.2 g/l. The saturation magnetization of 40.8 emu/g is high, considering that the ratio of FeCoNi to graphene is only 1 : 1 and heat treatment or high-temperature reduction processes were not applied. Compared with the saturation magnetization of previously reported magnetic@graphene hybrids (Ni@RGO (11.05 emu/g) [24] and FeNi@RGO (2 : 1, 21.1 emu/g) [30]) prepared via electroless plating, that of

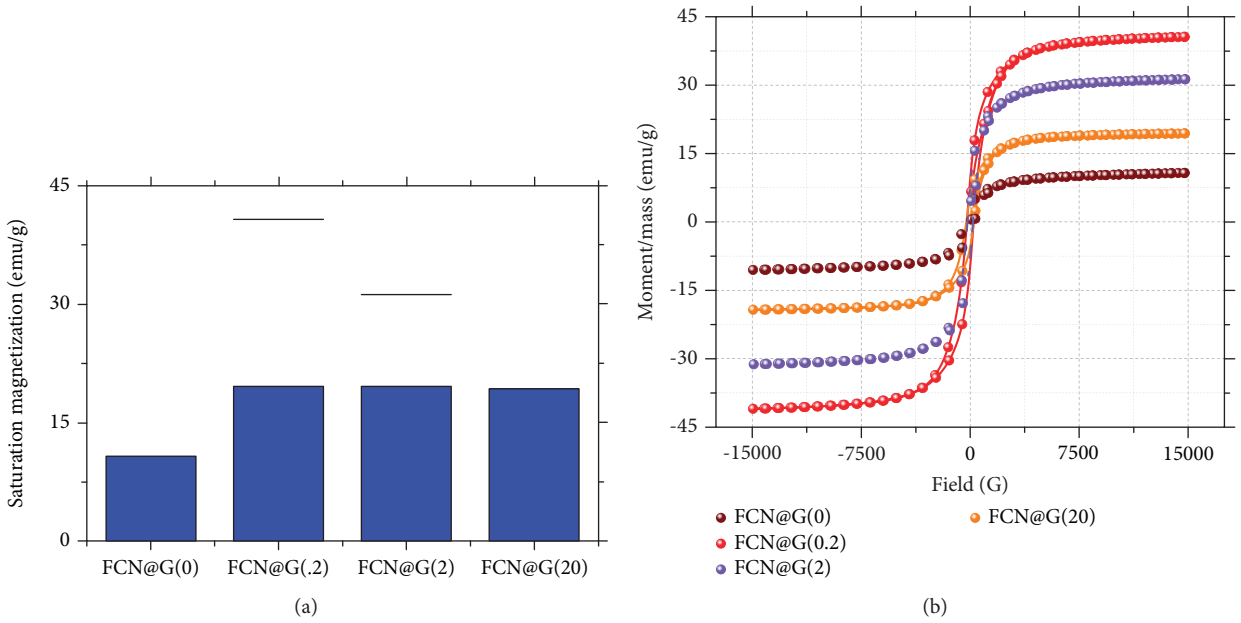

FIGURE 6: (a) Saturation magnetization values and (b) hysteresis loops of FeCoNi@graphene hybrids prepared under different pretreatment conditions.

FCN@G(0.2) was higher owing to the optimization of the sensitization process.

Consequently, to synthesize FeCoNi@graphene hybrids with a high saturation magnetization via electroless plating, the $SnCl_2$ solution concentration during sensitization should be low but not zero to reduce the excess residual SnO_2 and properly grow the Pd nanoparticles. The results indicate that the properties of other metal-graphene hybrid materials prepared via electroless plating can also be controlled.

4. Conclusions

We investigated the effect of sensitization on the morphological, structural, and magnetic properties of FeCoNi@graphene hybrids prepared by electroless plating. Because $SnCl_2$ is easily converted to Sn nanoparticles on the graphene surface, a high-concentration $SnCl_2$ solution generates excess SnO_2, thereby decreasing the saturation magnetization. In contrast, if sensitization is not performed, the growth of Pd proceeds in an entirely different manner. As a result, the obtained hybrid material exhibits a large amount of oxides and low magnetic property. Therefore, we can conclude that a low-concentration $SnCl_2$ solution is appropriate for the electroless plating of graphene. The characteristics of the nanoparticle@graphene hybrids obtained via electroless plating are significantly affected by sensitization because the growth behavior of Sn on graphene differs from that on the substrate used in conventional electroless plating owing to the large surface area of graphene. This study contributes to the synthesis of magnetic nanoparticle@graphene hybrids with the highest saturation magnetization based on a commercially available method. The mass-produced magnetic nanoparticle@graphene hybrids can be used for electromagnetic wave absorption in future studies.

Data Availability

The data used to support the findings of this study are available from the corresponding author upon request.

Conflicts of Interest

The authors declare that there is no conflict of interest regarding the publication of this paper.

Authors' Contributions

Kyunbae Lee and Taehoon Kim contributed equally to this work.

Acknowledgments

This research was supported by the Nano-Material Technology Development Program through the National Research Foundation of Korea (NRF) funded by the Ministry of Science, ICT, and Future Planning (No. 2016M3A7B4 900044). This research was also supported by the Fundamental Research Program (PNK5830) of the Korea Institute of Materials Science (KIMS).

References

[1] X. Li, J. Feng, Y. Du et al., "One-pot synthesis of $CoFe_2O_4$/graphene oxide hybrids and their conversion into FeCo/graphene hybrids for lightweight and highly efficient microwave absorber," *Journal of Materials Chemistry A*, vol. 3, no. 10, pp. 5535–5546, 2015.

[2] J. Lee, B. M. Jung, S. B. Lee, S. K. Lee, and K. H. Kim, "FeCoNi coated glass fibers in composite sheets for electromagnetic absorption and shielding behaviors," *Applied Surface Science*, vol. 415, pp. 99–103, 2017.

[3] R. Nicula, V. D. Cojocaru, M. Stir, J. Hennicke, and E. Burkel, "High-energy ball-milling synthesis and densification of Fe–Co alloy nanopowders by field-activated sintering (FAST)," *Journal of Alloys and Compounds*, vol. 434-435, pp. 362–366, 2007.

[4] A. L. Elías, J. A. Rodríguez-Manzo, M. R. McCartney et al., "Production and characterization of single-crystal FeCo nanowires inside carbon nanotubes," *Nano Letters*, vol. 5, no. 3, pp. 467–472, 2005.

[5] H. Wu, R. Zhang, X. Liu, D. Lin, and W. Pan, "Electrospinning of Fe, Co, and Ni nanofibers: synthesis, assembly, and magnetic properties," *Chemistry of Materials*, vol. 19, no. 14, pp. 3506–3511, 2007.

[6] C. Wang, R. Lv, Z. Huang, F. Kang, and J. Gu, "Synthesis and microwave absorbing properties of FeCo alloy particles/graphite nanoflake composites," *Journal of Alloys and Compounds*, vol. 509, no. 2, pp. 494–498, 2011.

[7] H. Wang, D. Zhu, W. Zhou, and F. Luo, "Enhanced microwave absorbing properties and heat resistance of carbonyl iron by electroless plating Co," *Journal of Magnetism and Magnetic Materials*, vol. 393, pp. 445–451, 2015.

[8] Y. P. Wu, G.-C. Han, and L. B. Kong, "Microstructure and microwave permeability of FeCo thin films with Co underlayer," *Journal of Magnetism and Magnetic Materials*, vol. 322, no. 21, pp. 3223–3226, 2010.

[9] Y. Zhang, T. Zuo, Y. Cheng, and P. K. Liaw, "High-entropy alloys with high saturation magnetization, electrical resistivity, and malleability," *Scientific Reports*, vol. 3, no. 1, p. 1455, 2013.

[10] Q. Li, X. Li, S. Wageh, A. A. Al-Ghamdi, and J. Yu, "CdS/graphene nanocomposite photocatalysts," *Advanced Energy Materials*, vol. 5, no. 14, 2015.

[11] C.-C. Yeh and D.-H. Chen, "Ni/reduced graphene oxide nanocomposite as a magnetically recoverable catalyst with near infrared photothermally enhanced activity," *Applied Catalysis B: Environmental*, vol. 150-151, pp. 298–304, 2014.

[12] K. Chokprasombat, S. Pinitsoontorn, and S. Maensiri, "Effects of Ni content on nanocrystalline Fe–Co–Ni ternary alloys synthesized by a chemical reduction method," *Journal of Magnetism and Magnetic Materials*, vol. 405, pp. 174–180, 2016.

[13] Q.-h. Hu, X.-t. Wang, H. Chen, and Z.-f. Wang, "Synthesis of Ni/graphene sheets by an electroless Ni-plating method," *New Carbon Materials*, vol. 27, no. 1, pp. 35–41, 2012.

[14] X.-W. Liu, J.-J. Mao, P.-D. Liu, and X.-W. Wei, "Fabrication of metal-graphene hybrid materials by electroless deposition," *Carbon*, vol. 49, no. 2, pp. 477–483, 2011.

[15] S. M. Popescu, A. J. Barlow, S. Ramadan, S. Ganti, B. Ghosh, and J. Hedley, "Electroless nickel deposition: an alternative for graphene contacting," *ACS Applied Materials & Interfaces*, vol. 8, no. 45, pp. 31359–31367, 2016.

[16] X. Yin, L. Hong, B. H. Chen, and T. M. Ko, "Modeling the stability of electroless plating bath—diffusion of nickel colloidal particles from the plating frontier," *Journal of Colloid and Interface Science*, vol. 262, no. 1, pp. 89–96, 2003.

[17] I. Arief, S. Biswas, and S. Bose, "FeCo-anchored reduced graphene oxide framework-based soft composites containing carbon nanotubes as highly efficient microwave absorbers with excellent heat dissipation ability," *ACS Applied Materials & Interfaces*, vol. 9, no. 22, pp. 19202–19214, 2017.

[18] L. Nan, Z. Fan, W. Yue et al., "Graphene-based porous carbon-Pd/SnO_2 nanocomposites with enhanced electrocatalytic activity and durability for methanol oxidation," *Journal of Materials Chemistry A*, vol. 4, no. 22, pp. 8898–8904, 2016.

[19] M. Uysal, H. Akbulut, M. Tokur, H. Algül, and T. Çetinkaya, "Structural and sliding wear properties of Ag/Graphene/WC hybrid nanocomposites produced by electroless co-deposition," *Journal of Alloys and Compounds*, vol. 654, pp. 185–195, 2016.

[20] C. Zhao and J. Wang, "Fabrication and tensile properties of graphene/copper composites prepared by electroless plating for structural applications," *Physica Status Solidi (A)*, vol. 211, no. 12, pp. 2878–2885, 2014.

[21] C.-C. Chou, C.-H. Hsieh, and B.-H. Chen, "Hydrogen generation from catalytic hydrolysis of sodium borohydride using bimetallic Ni–Co nanoparticles on reduced graphene oxide as catalysts," *Energy*, vol. 90, pp. 1973–1982, 2015.

[22] P. Zhao, W. Yue, X. Yuan, and H. Bao, "Exceptional lithium anodic performance of Pd-doped graphene-based SnO_2 nanocomposite," *Electrochimica Acta*, vol. 225, pp. 322–329, 2017.

[23] P. Zhao, W. Yue, Z. Xu, S. Sun, and H. Bao, "Graphene-based Pt/SnO_2 nanocomposite with superior electrochemical performance for lithium-ion batteries," *Journal of Alloys and Compounds*, vol. 704, pp. 51–57, 2017.

[24] Y. Wang, Y. Zhao, T. Bao, X. Li, Y. Su, and Y. Duan, "Preparation of Ni-reduced graphene oxide nanocomposites by Pd-activated electroless deposition and their magnetic properties," *Applied Surface Science*, vol. 258, no. 22, pp. 8603–8608, 2012.

[25] X. Wei and D. K. Roper, "Tin sensitization for electroless plating review," *Journal of the Electrochemical Society*, vol. 161, no. 5, pp. D235–D242, 2014.

[26] X. Chen, G. Wu, J. Chen, X. Chen, Z. Xie, and X. Wang, "Synthesis of "clean" and well-dispersive Pd nanoparticles with excellent electrocatalytic property on graphene oxide," *Journal of the American Chemical Society*, vol. 133, no. 11, pp. 3693–3695, 2011.

[27] X. Li and S. Takahashi, "Synthesis and magnetic properties of Fe–Co–Ni nanoparticles by hydrogen plasma–metal reaction," *Journal of Magnetism and Magnetic Materials*, vol. 214, no. 3, pp. 195–203, 2000.

[28] K. V. P. M. Shafi, A. Gedanken, R. Prozorov, and J. Balogh, "Sonochemical preparation and size-dependent properties of nanostructured $CoFe_2O_4$ particles," *Chemistry of Materials*, vol. 10, no. 11, pp. 3445–3450, 1998.

[29] L. Li, G. Li, R. L. Smith, and H. Inomata, "Microstructural evolution and magnetic properties of $NiFe_2O_4$ nanocrystals dispersed in amorphous silica," *Chemistry of Materials*, vol. 12, no. 12, pp. 3705–3714, 2000.

[30] B. Zhang, J. Wang, H. Tan et al., "Synthesis of Fe@Ni nanoparticles-modified graphene/epoxy composites with enhanced microwave absorption performance," *Journal of Materials Science: Materials in Electronics*, vol. 29, no. 4, pp. 3348–3357, 2018.